Geosynthetics - 7th ICG - Delmas, Gourc & Girard (eds) © 2002 Swets & Zeitlinger, Lisse ISBN 90 5809 523 1

FEM simulation of failure of reinforced sand in plane strain compression

F.L. PENG, Technical Development Division, Shiraishi Corporation, Tokyo, Japan
(formerly Graduate Student at the University of Tokyo)
F. TATSUOKA, Department of Civil Engineering, University of Tokyo, Tokyo, Japan
M. S. A. SIDDIQUEE, Department of Civil Engineering, Bangladesh University of E&T, Dhaka, Bangladesh
N. KOTAKE, Civil Design Division, Toyo Construction Co., Ltd., Tokyo, Japan

ABSTRACT: To gain a better insight into the failure mechanism of reinforced sand, results from plane strain compression tests of dense Toyoura sand reinforced with planar reinforcement having a wide range of stiffness were simulated by a nonlinear FEM. The analysis incorporated an energy-based elasto-viscoplastic constitutive model for sand developed to have a stress path-independent work-hardening parameter based on the modified plastic strain energy concept. The constitutive model takes into account the nonlinear viscous property of sand based on a non-linear three-component rheology model. Results from tests on sand specimens reinforced by using relatively flexible and rigid reinforcement as well as an unreinforced sand specimen are well simulated giving a deep insight into the failure of reinforced sand.

1 INTRODUCTION

Kotake et al. (1999) successfully simulated the results of plane strain compression (PSC) tests on small specimens of dense Toyoura sand that were either unreinforced or tensile-reinforced with various types of planar-reinforcements placed horizontal (Tatsuoka and Yamauchi, 1986). They used the nonlinear elasto-plastic FEM incorporating the plastic shear strain-hardening proposed by Tatsuoak et al. (1993). In the results of their numerical analysis of the reinforced specimens, however, the maximum stress ratio and pre-peak stiffness are noticeably larger in the FEM analysis than in the experimental PSC tests. This discrepancy is due, at least partly, to the following reasons (Yasin and Tatsuoka, 2000; Peng et al., 2000):

1) The plastic shear strain-hardening model was constructed based on the results from conventional PSC tests at constant confining pressure.
2) As the FEM analysis revealed (Kotake et al., 1999; Peng et al., 2000), typical stress paths inside the reinforced specimens are similar to anisotropic compression stress paths at high stress ratios close to that at failure, which are considerably different from those in the conventional PSC tests.

The objective of this study is, therefore, to re-simulate the results from a series of PSC tests on unreinforced and reinforced dense Toyoura sand specimen (Tatsuoka and Yamauchi, 1986) based on a new constitutive model for sand. The simulation was based on a new elasto-viscoplastic constitutive model using a strain energy-hardening function that was introduced to overcome the above-mentioned drawback. The new constitutive model also considers the stress history- and stress path-dependency of the deformation characteristics of sand. The viscous property was introduced aiming at: 1) a better stability in the numerical simulations; and 2) simulations of loading rate effects and creep deformation of reinforced sand. Discussions on the second issue are beyond the scope of this paper.

2. PSC TESTS ON REINFORCED SAND

In the physical PSC tests, a planar tensile reinforcing member was placed horizontal at the mid-height of specimens that were 7.5, 8.0 and 4.0 cm in the directions of σ_1 , σ_2 and, σ_3 having an initial void ratio e_o equal to 0.66 (Figure 1). The surfaces of the σ_1 and σ_2 planes were well-lubricated (Tatsuoka et al., 1984), while the measured boundary stresses were corrected for membrane forces and vertical friction working on the confining platens. The details are described in Tatsuoka and Yamauchi (1986). In the present study, the following three typical tests were analysed:

1) Unreinforced specimen;
2) Specimen reinforced by using relatively flexible reinforcement, a urethane sheet.
3) Specimen reinforced with rigid rough reinforcement, a rough brass plate having surfaces roughened by gluing sand particles.

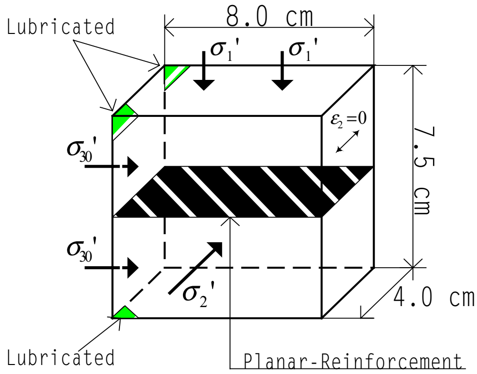

Figure 1. Reinforced sand specimen for PSC tests

3. FEM DETAILS

3.1 *Modeling of PSC specimen*

The PSC specimen was discretised into 0.4 cm x 0.4 cm square plane strain elements with a number of total nodal points of 441 (Figure 2). The urethane sheet was modeled by 20 linear-elastic truss elements having only an axial stiffness (EA= 4.51 x 10^{+1} kN/m), while the rough-brass plate was modeled by 20 linear-elastic truss elements having an axial stiffness (EA= 5.05 x 10^{+4} kN/m) and a bending stiffness (EI= 1.05 x 10^{-3} kNm^2/m). No interface elements were used, since no noticeable slippage between the reinforcement and sand was observed in these PSC tests.

Initial isotropic effective confining pressure of σ_c (= 49 *kPa*) was first given to all the plane strain elements. A displacement increment of 0.0005×2 cm/step, i.e., an average axial strain increment d ε_a of 0.0132 %/step, was applied, which has been found to be small enough to keep accuracy and numerical stability with an equilibrium iteration tolerance of a force norm as well as a energy norm ε_E of 10^{-6}. A set of non-linear equations was solved by the Dynamic

Relaxation technique (Tanaka and Kawamoto, 1988; Tanaka and Sakai, 1993), which has a reputation in solving highly non-linear equations, especially for high friction angle materials as in the present case. The integration of the elasto-plastic equation was done by the Return Mapping scheme (Ortiz and Simo, 1986), which is a first order approximated Euler backward integration. The detail is described in Siddiquee et al. (1995, 1999).

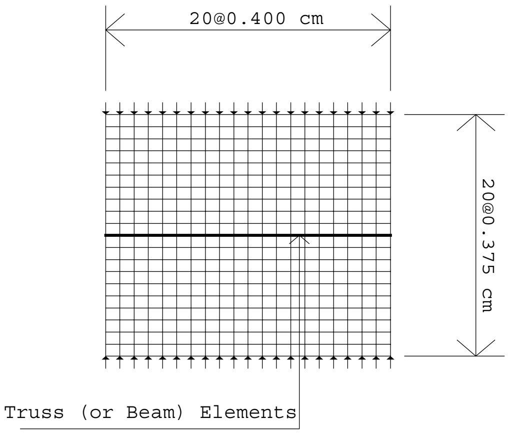

Figure 2. FEM mesh

3.2 *Constitutive model for sand*

In the elasto-plastic constitutive model for sand that was originally developed by Siddiquee (1994) and Siddiquee et al. (1995), the inherent and stress system-induced cross-anisotropic elasticity is considered, based on results with respect to anisotropic elastic deformation properties of sand from a series of laboratory stress-strain tests (Hoque and Tatsuoka, 1996;1998). The model is coupled with an isotropically work-hardening and softening, non-associated, elasto-plastic material description. The yield function and the plastic potential function are of, respectively, Mohr-Coulomb and Drucker-Prager type. It is assumed that the deformation of a given sand element under uniform boundary stress conditions is homogeneous in the pre-peak regime, while strain localization into a shear band starts suddenly at the peak stress state. A smear method, which is similar to the one proposed by Pietruszczak and Mroz (1981), was employed to incorporate strain localization (Tanaka and Sakai, 1993). Unlike their method, however, no direction of shear banding was specified.

In the present study, the original model was first modified by incorporating the modified plastic strain energy concept (Peng, 2000; Peng et al., 2000, 2001, 2002). The modified plastic strain energy concept is represented by a unique relationship between the modified plastic strain energy and a stress parameter, which is independent of stress history. This concept was developed based on results from a series of drained PSC tests performed along various stress paths on saturated dense Toyoura sand with accurate stress and strain measurements (Yasin and Tatsuoka, 2000). The new constitutive model is capable of simulating the effects on the deformation characteristics of stress path as well as pressure level (Yasin and Tatsuoka, 2000; Peng et al., 2000, 2001).

Figure 3 shows the three-component model that was developed to simulate the viscous features of the stress-strain behaviour of geomaterials (Di Benedetto et al., 2001; Tatsuoka et al., 2001) and employed in the present study. In the framework of the three-component model, the conventional elasto-plastic model consists of the two components (**E** + **F**) depicted in Figure 3, where **E** means the hypo-elastic component, while **F** means the non-linear inviscid component, for which the stress is a unique function of irreversible strain in the monotonic loading case. Di Benedetto et al. (2001) and Tatsuoka et al. (2001) showed that the three-component model can simulate very well the viscous property of sand, such as; a) effects of gradual and stepwise changes in the strain rate and different constant strain rates on monotonic loading stress-strain behaviour; b) creep, where the irreversible strain rate continuously decreases at a constant stress; c) stress-relaxation, where the stress decreases while the irreversible strain rate continuously decreases at a constant total strain with negative elastic strain rates; and so on.

In summarizing the above, the modified constitutive model incorporates the following properties:

a) the inviscid pre-peak stress-strain relation with work-hardening elasto-plastic deformation characteristics;
b) a non-associated flow for irreversible strain;
c) anisotropic strength and deformation;
d) pressure level-dependency of strength and deformation;
e) post-peak work-softening;
f) shear banding with a characteristics shear band width (i.e., particle size effect); and
g) viscous deformation properties of sand.

The FEM code incorporating the above-proposed model has been validated by a direct comparison between results from the numerical on analysis using a single element and physical test results (Siddiquee and Tatsuoka, 2001).

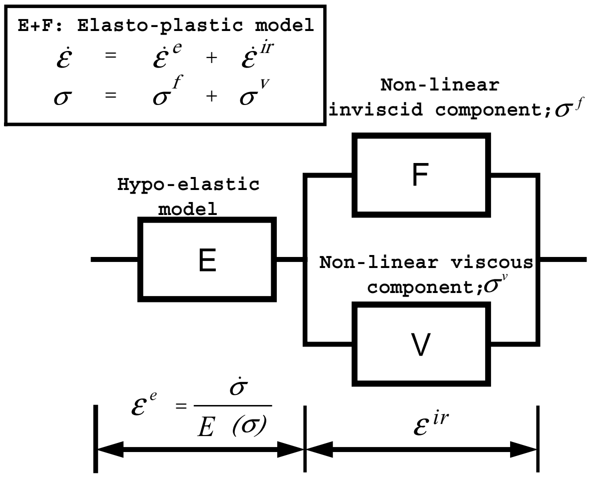

Figure 3. Three-component elastic-viscous-plastic model

In the present simulation, loading was made at a constant displacement rate equal to 0.15 mm/min referencing to the physical model test. It was found that the viscous stress always occupied very small part of the total stress. Despite the above, the numerical solution became substantially stable by introducing viscous effects when compared with the previous analysis.

4. RESULTS AND DISCUSSIONS

4.1 *Global Stress-Strain Relationship*

The global relationships between the boundary principal stress ratio R^* $(=\sigma_1/\sigma_c)$ and the average axial strain ε_a from the FEM analysis and the experimental PSC tests are compared in Figure 5. The following trends of behaviour may be seen:

1) For all the three test cases, the proposed FEM analysis method can simulate very well the physical test results not only at pre-peak but also at post peak regime for widely different reinforcing effects.
2) Despite the above, the agreement for the post-peak stress-strain behaviour is relatively low, showing that the present analysis method has still some limitation.

4.2 *Local Characteristics and Shear Band*

The contours of incremental local maximum shear strains $\gamma_{max}=\varepsilon_1-\varepsilon_3$ observed between two successive loading stages in the experimental PSC tests are shown in Figure 6. These strain values were obtained by reading displacements of targets located at a vertical and horizontal spacing of 5 mm that had been printed on the specimen rubber membrane of the intermediate principal stress surface. To this end, a number of pictures were taken during the respective PSC test. The representative loading stages selected were " before peak (A)", "around peak (B)" and "after peak to residual (C)" as denoted in Figure 5. The corresponding contours of γ_{ma} obtained from the FEM analyses are shown in the Figure 5.

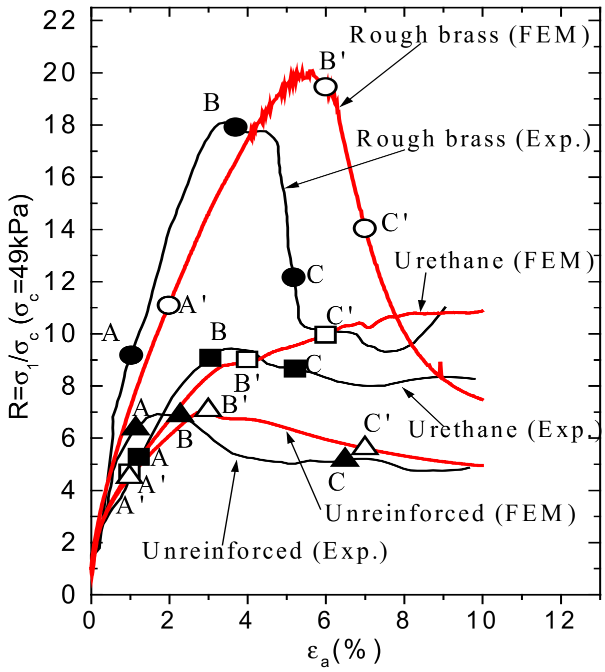

Figure 4 Global stress-strain relations

It may be seen from Figure 5 that the development of shear band, which affected the global stress-strain behavior, observed in the experimental PSC tests was well simulated by FEM analysis: that is:

1) In the physical test on the unreinforced specimen, a V-shaped shear band, reflecting at the bottom of the specimen, started appearing around the peak stress state, as seen from the incremental γ_{max} field (A→B). Then, the strain was localized more intensely into the shear band in the post-peak regime (B→C). Also in the FEM analysis, a V-shape shear band started appearing around the peak state (A'→B'), which developed further, reflecting clearly at the specimen bottom in the post-peak regime (B'→C').
2) The general pattern of shear banding between stages A and B in the physical test on the specimen reinforced with urethane was similar to the one in the unreinforced case. In addition, the shear band penetrated through the reinforcement, perhaps due to the flexible nature of the reinforcement. However, the strain was less localized into the respective shear band while more shear bands developed in the specimen reinforced with urethane. This was likely due to the restraint by reinforcement to the free development of shear band. By this interaction, relatively large tensile strains (hence tensile stresses) were induced in the reinforcement at large average strains.
3) For the specimen reinforced with rough brass, up to the peak state (A→B and A'→B'), very small shear strains were induced in the vicinity of the rough brass due to its high confining effect, while the strain started localizing to some extent around both ends of the reinforcement. After peak (B→C and B'→C'), a greatly intense strain localization into a V-shaped

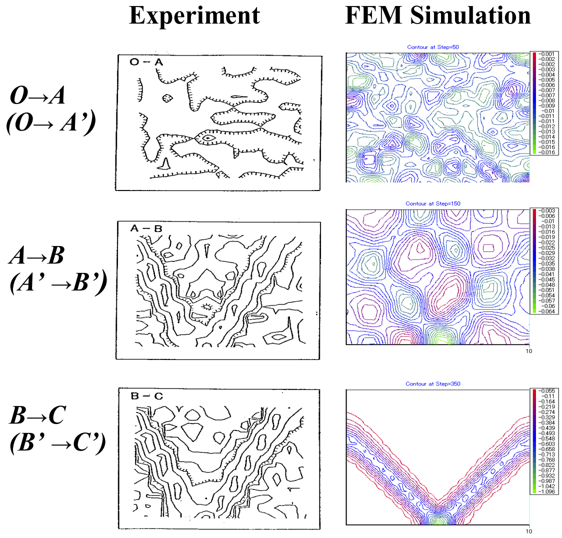

(a) Unreinforced

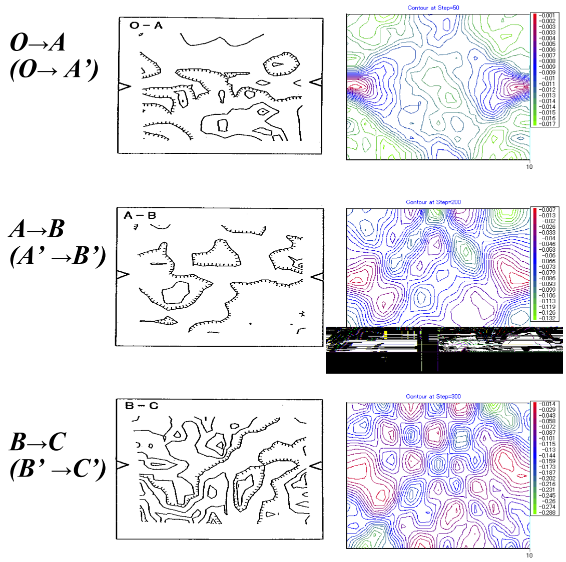

(b) Urethane-reinforced

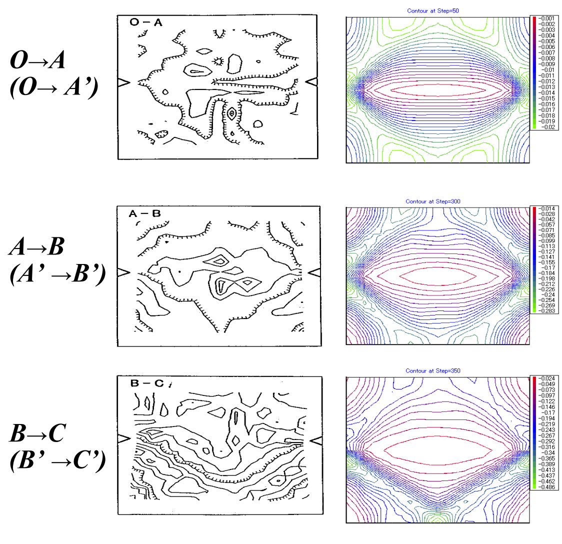

(c) Rough brass--reinforced

Figure 5 Contours of incremental local maximum shear strain shear band developed in the bottom half of the specimen with sharp reflection at the bottom end. Then, strain localized into a shear band while the reminder behaved like a rigid body. Due to a high rigidity of the brass reinforcement, the shear band could not penetrate the reinforcement, and shear banding developed in the zones away from the reinforcement.

5. CONCLUSIONS

From the results presented above, the following conclusions can be derived:

1)The relevant FEM analysis could simulate very well not only the global stress-strain behavior but also the local deformation pattern of both unreinforced sand specimen and those reinforced with a wide variety of planar reinforcement, flexible and rigid, which are brought to failure in plane strain compression tests. The simulation of strain localization into a shear band (or shear bands) is one of the keys for the success of such a numerical simulation.

2)The FEM analyses could well simulate the failure mechanism associated with shear banding of unreinforced sand specimens and those reinforced with flexible and rigid reinforcement. By an insight into the strain fields, the reinforcing mechanism by tensile reinforcement was clearly understood in relation to the global stress-strain relations.

3)The degree of simulation was improved by incorporating the work-hardening function, in place of the shear strain-hardening function in the previous simulation.

4)In the present simulation of PSC tests performed at a constant strain rate, the viscous stress was always negligible when compared with the total stress. Despite the above, by incorporating the viscous property in the constitutive model of sand, the simulation became much more stable, in particular in the post-peak regime, when compared with the previous simulation based on the elasto-plastic model for sand.

REFERENCES

Di Benedetto,H., Tatsuoka,F. and Ishihara,M. 2001. Time- dependent shear deformation characteristics of sand and their constitutive modeling. *Soils and Foundations* (accepted).

Flanagan,D.P. and Belytschko,T. 1981. A uniform strain hexahedron and quadrilateral with orthogonal hourglass control. *Int. J. Numer. Methods Eng*., Vol.17, pp.679-706.

Hoque,E., Tatsuoka,F. and Sato,T. 1996. Measuring anisotropic elastic properties of sand using a large triaxial specimen. *Geotechnical Testing Journal, ASTM,* Vol.19, No.4, pp.411-420.

Hoque,E., and Tatsuoka,F. 1998. Anisotropy in the elastic deformation of materials. *Soils and Foundations,* Vol.38, No.1, pp.163-179.

Kotake,N., Peng,F.L., Tanaka,T., Higuchi,T., Shida,Y., Yanagisawa,H. and Tatsuoka,F. 1997. Numerical simulation of plane strain compression tests on large geogrid-reinforced sand specimens. *Geosynthetics Engineering Journal*, Japan Chapter of IGS, Vol.12, pp.36-44.

Kotake,N. 1998. FEM simulation of deformation and failure of reinforced soil. *Doctoral Thesis*, the University of Tokyo, Japan.

Kotake,N., Tatsuoka,F., Tanaka,T., Siddiquee, M.S.A. and Yamauchi,H. 1999. An insight into the failure of reinforced sand in plane strain compression by FEM simulation. *Soils and Foundations*, Vol.39, pp.39-

Ortiz,M. and Simo,J.C. 1986. An analysis of a new class of intergration algorithms for elasto-plastic constitutive relations. *Int. J. Numer. Methods Eng*., Vol.23, pp. 53-366.

Peng,F.L. 2000. Constitutive Modeling and Finite Element Analysis of Reinforced soils. *Ph. D. Thesis*, the University of Tokyo.

Peng,F.L., Kotake,N, Tatsuoka,F., Hirakawa,D. and Tanaka,T. 2000. Plane strain compression behavior of geogrid-reinforced sand and its numerical analysis. *Soils and Foundations*, Vol.40, N0.3, pp.55-74.

Peng,F.L., Tatsuoka,F., Siddiquee,M.S.A., Kotake,N., and Yamauchi,H. 2000. FEM simulation of Failure of reinforced sand based on a new work-hardening constitutive model. *Geosynthetics Engineering Journal*, JCIGS, Vol.15, pp.166-175.

Peng,F.L., Tatsuoka,F., Siddiquee,M.S.A. and Yasin, S.J.M. 2001. A new plastic model for granular materials. *Proc. of the 10th International Conference on Computer Methods and Advances in Geomechanics* (Desai et al. eds), Arizona, Vol.1, pp.383-388.

Peng,F.L., Tatsuoka,F., Siddiquee,M.S.A. 2002. An energy-based modeling of sand and its FEM application. *Proc. of the 15th ASCE Engineering Mechanics Conference,* ASCE, New York (accepted).

Pietruszczak, S. T. and Mroz, Z. 1981. Finite element analysis of deformation of strain softening material. *Int. J. Numer. Methods Engrg*., Vol. 17, pp. 327-334.

Siddiquee,M.S.A. 1994. Finite Element analysis of settlement and bearing capacity of footing on sand. *Doctor's Thesis*, the University of Tokyo.

Siddiquee,M.S.A., Tanaka,T. and Tatsuoka,F. 1995. Tracing the equilibrium path by dynamic relaxation in materially non-linear problems. *International Journal for Numerical and Analytical Methods in Geomechanics*, Vol.19, pp.749-767.

Siddiquee, M. S. A., Tanaka, T., Tatsuoka, F., Tani, K. and Morimoto, T. 1999. FEM simulation of scale effect in bearing capacity of strip footing on sand. *Soils and Foundations*, Vol.39, No.4, pp.91-109.

Siddiquee,M.S.A. and Tatsuoka,F. 2001. Modeling time-dependent stress-strain behavior of stiff geo-materials and its application. *Proc. of the 10^{th} International Conference on Computer Methods and Advances in Geomechanics* (Desai et al. eds), Arizona, Vol.1, pp.401-406.

Tanaka,T. and Kawamoto,O. 1988. Three dimensional finite element collapse analysis for foundations and slopes using dynamic relaxation. *Proc. of Numerical Methods in Geomechanics*, Insbruch, pp.1213-1218.

Tanaka,T. and Sakai,T. 1993. Progressive failure and scale effect of trap-door problems with granular materials. *Soils and Foundation*, Vol.33, No.1, pp.11-22.

Tatsuoka,F. and Yamauchi,H. 1986. A reinforcing method for steep clay slopes with a non-woven fabric. *Geotextiles and Geomembranes*, Vol.4, No.3/4, pp.241-268

Tatsuoka,F., Molenkamp,F., Torii,T. and Hino,T. 1984. Behaviour of lubrication layers of platens in element tests. *Soils and Foundations*, Vol.24, No.1, pp.113-128.

Tatsuoka,F., Siddiquee,M.S.A., Park,C.-S., Sakamoto,M. and Abe,F. 1993. Modeling stress-strain relations of sand. *Soils and Foundations*, Vol.33, No.2, pp.60-81.

Tatsuoka,F., Ishihara,M., Di Benedetto,H. and Kuwano, R. 2001. Time-dependent shear deformation characteristics of geo-materials and their simulation. *Soils and Foundations* (accepted).

Yasin,S.J.M. and Tatsuoka,F. 2000. Stress history-dependent deformation characteristics of dense sand in plane strain. Soils and Foundations, Vol. 40, No. 2, pp. 77-98.